BUDOWNICTWO
CZASOPISMO TECHNICZNE
TECHNICAL TRANSACTIONS
CIVIL ENGINEERING
WYDAWNICTWO POLITECHNIKI KRAKOWSKIEJ
1-B/2011
ZESZYT 3
ROK 108
ISSUE 3
YEAR 108

MAGDALENA GERMAN*, ADAM ZABORSKI**

NUMERICAL ANALYSIS OF CHLORIDE CORROSION OF REINFORCED CONCRETE

ANALIZA NUMERYCZNA KOROZJI CHLORKOWEJ W ELEMENTACH ŻELBETOWYCH

Abstract

The phenomenon of corrosion can be divided in two stages: the initiation and propagation phases. The initiation phase analysis considers a chloride ions flux described by Nernst--Planck equation. Following the results of initiation phase, a numerical analysis of corrosion propagation phase has been performed. The propagation phase is the time, when corrosion cell is formed. As a result of current flowing through reinforcement, the corrosion products are accumulated at the steel-concrete interface, what generates the tensile stresses in concrete, causing cracking. On the surface longitudinal cracks and concrete splitting are observed. This leads to the loss of strength of the element.

Keywords: reinforced concrete, chloride corrosion, corrosion initiation phase, corrosion cell, corrosion current, corrosion propagation phase, cracking

Streszczenie

Zjawisko korozji może być podzielone na dwa etapy: inicjacji i propagacji. Analiza fazy inicjacji obejmuje dotyczy przepływu jonów chlorkowych, który został opisany równaniem Nernsta-Plancka. Na podstawie uzyskanych rezultatów dokonano analizy fazy propagacji korozji. Podczas fazy propagacji korozji utworzone zostaje ogniwo korozyjne, w wyniku czego przez zbrojenie przepływa prąd. Pręt zbrojeniowy ulega korozji, a jej produkty są gromadzone na styku stal-beton. W betonie generowane są naprężenia rozciągające, powodujące zarysowanie widoczne na powierzchni betonu. Korozja chlorkowa prowadzi do zarysowanie, odprysków betonu, utraty przyczepności między stalą i betonem oraz utratą nośności elementu.

Słowa kluczowe: żelbet, korozja chlorkowa, faza inicjacji korozji, ogniwo korozyjne, prąd korozyjny, faza propagacji korozji, zarysowanie

* Mgr inż. Magdalena German, Institute for Computational Civil Engineering, Faculty of Civil Engineering, Cracow University of Technology.
** Dr inż. Adam Zaborski, Institute of Structural Mechanics, Faculty of Civil Engineering, Cracow University of Technology.

1. Introduction

It has been assumed to describe the process of chloride corrosion by the two-stage Tuutti's model, which is presented in fig. 1. The stages can be characterized as initiation and propagation phases. During the initiation phase chlorides penetrate concrete cover and gather around reinforcement bars, lowering pH of the concrete. As time passes by, chloride concentration in concrete increases until it reaches a chloride threshold value. The moment of reaching the threshold is the moment when the initiation phase ends and the propagation stage begins. During the propagation phase steel loses its passive layer and a corrosion current starts to flow. Stresses, caused by a growing amount of corrosion products, appear in the element. The corrosion process leads to cracking, splits, delamination, loss of strength and general failure of the element.

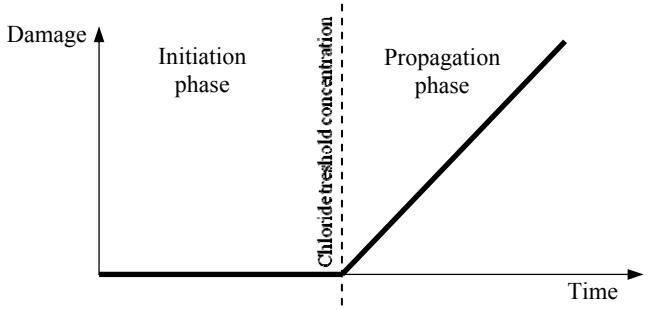

Fig. 1. Two-stage Tuutti's model

Rys. 1. Dwuetapowy model Tuuttiego

2. Chloride ions flux

Chloride ions present in the environment permeate into the element. In case of uncracked concrete surface, the total ion flux is caused by two driving forces – concentration gradient and electrical potential gradient. The concentration gradient causes diffusion flux, whereas the electrical potential gradient causes the migration flux. During the diffusion process, some ions tend to diffuse at higher rate. However, any excess charge transferred by the faster ions builds up a local electric field, which slows down the faster ions, and accelerates the slower ions [1, 2]. The total chloride ion flux **J** can be described by the Nernst-Planck equation [1]

$$\mathbf{J} = -D_c \operatorname{grad}\left(C_f\right) + \frac{zFD_c}{RT} C_f \operatorname{grad}\left(E_{\mathrm{Cl}}\right) \tag{1}$$

where:

C_f – concentration of free chloride ions,
D_c – chloride diffusion coefficient,
z – valence of the chloride ion,
F – Faraday constant,

E_{Cl} – electric field potential for chlorides,
R – ideal gas constant,
T – temperature.

During the initiation process a part of chlorides reacts with hydratation products and cement. Only the free chlorides cause the corrosion of the reinforcement [5, 8]. The total chloride concentration is a sum of free and bound chlorides. The amount of free chlorides can be determined using Freundlich isotherm. The equilibrium between bound chloride ions C_b and free chloride ions C_f, is then expressed by [5]

$$C_b = \alpha C_f^{\beta} \tag{2}$$

where:
α, β – empirical constants.

The electrical potential set up by drifting ions can be determined on the basis of the Poisson equation [2]

$$\nabla^2 E_{Cl} = \frac{Fz \cdot C(\bar{x}, t)}{\varepsilon} \tag{3}$$

where:
ε – dielectric constant of the medium.

The equation of mass conservation can be written as

$$\frac{\partial C(\bar{x}, t)}{\partial t} + \mathrm{div}(\mathbf{J}) = 0 \tag{4}$$

with the boundary conditions specified as follows

$$C(\bar{x}, t) = 0 \text{ when } t = 0 \tag{5}$$

$$C(\bar{x}, t) = C_0 \text{ for } \bar{x} \in \Gamma \tag{6}$$

This procedure is applicable only in case of uncracked concrete. The cracked concrete cannot be treated as a homogenous porous material and the rate of migration of chloride ions towards the reinforcement is additionally dependent on crack characteristics.

3. Corrosion current

When the chloride threshold value is reached by the free chlorides concentration at the reinforcement level, steel becomes active, and corrosion cell is formed. Due to difference in electrical potential between anode and cathode, a corrosion current starts to flow. Iron is oxidized to ferrous ions at the anode and the oxygen is reduced releasing hydroxyl ions at the cathode.

$$2\mathrm{Fe} \rightarrow 2\mathrm{Fe}^{2+} + 4e^{-} \tag{7}$$

$$\mathrm{O}_2 + 2\mathrm{H}_2\mathrm{O} + 4e^{-} \rightarrow 4\mathrm{OH}^{-} \tag{8}$$

The current flowing cause the polarization of cathode and anode areas, and the difference in potentials is known as overpotential. The relation between half-cell potential and corrosion current flowing through it, forms the polarization curve of electrode, known as the Evans diagram [8, 9].

To break the resistance during ion transfer at the anode and cathode, an external activation energy need to be supplied. This results in activation overpotential at the anode and cathode, expressed by [9]

$$i_a = i_{oa} \exp\left(\frac{E - E_a^0}{\beta_a}\right) \tag{9}$$

$$i_c = i_{oc} \frac{C_{ox}}{C_{ox}^s} \exp\left(\frac{E_c^0 - E}{\beta_c}\right) \tag{10}$$

where:

$E_a^0 = -0.440$ V – standard potential in anodic reaction,
$E_c^0 = 0.401$ V – standard potential in cathodic reaction,
i_a – current density for iron oxidation reaction,
i_c – current density for oxygen reduction reaction,
i_{oa} – exchange current density for iron dissolution, taken as $3.75 \cdot 10^{-4}$ A/m^2,
i_{oc} – exchange current density for the cathodic reaction, taken as $1.25 \cdot 10^{-5}$ A/m^2,
β_a – activation Tafel slope for the anodic reaction,
β_c – activation Tafel slope for the cathodic reaction,
C_{ox} – dissolved oxygen concentration at the steel surface,
C_{ox}^s – dissolved oxygen concentration at the external concrete surface.

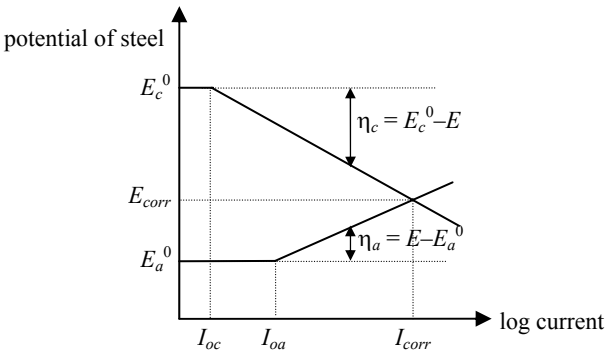

Fig. 2. Evans diagram for the anodic and cathodic process

Rys. 2. Diagram Evansa dla procesów anodowych i katodowych

Equation (10) considers difference in oxygen concentration at the steel surface and external concrete surface. In case of anodic reaction, change of concentration of reduced substance can be neglected, due to unlimited iron supply [8].

As a result of polarization caused by current flowing between anode and cathode, the potentials of electrode become equal and the reinforcing steel is freely corroding. The new potential, called corrosion potential E_{corr} is a value, for which oxidation and reduction reactions rates are equal. The corrosion potential E_{corr} and corrosion current density i_{corr} (in A/m^2) can be defined also by intersection of anodic and cathodic branches of the polarization curves at fig. 2. This intersection point represents conditions at which the anodic and cathodic currents are equal (but opposite in polarity) [8, 9]

$$I_{corr} = i_a \cdot A_a = i_c \cdot A_c \tag{11}$$

where:

I_{corr} – corrosion current,
A_a – anode area,
A_c – cathode area.

By substituting equations (9) and (10) into equation (11), the corrosion potential can be expressed by

$$E_{corr} = \frac{1}{\beta_a + \beta_c}\left(\beta_a\beta_c \ln\left(\frac{i_{oc}C_{ox}A_c}{i_{oa}C_{ox}^s A_a}\right) + \beta_c E_a^0 + \beta_a E_c^0\right) \tag{12}$$

4. Oxygen flux

Cathodic reaction depends on oxygen concentration C_{ox}. While corrosion proceeds, initial supply available in concrete gets exhausted, and oxygen must be transported into the cross-section. To describe total oxygen flux $\mathbf{J}_{ox}$ Fick's equation can be used

$$\mathbf{J}_{ox} = -D_{ox}\,\mathrm{grad}\left(C_{ox}\right) \tag{13}$$

where:

D_{ox} – diffusion coefficient for oxygen.

Thus for oxygen, the equation of mass conservation can be written as follows

$$\frac{\partial C_{ox}\left(\bar{x},t\right)}{\partial t} + \mathrm{div}\left(\mathbf{J}_{ox}\right) = 0 \tag{14}$$

with the boundary conditions

$$C_{ox}\left(\bar{x},t\right) = 0.005 \text{ when } t = 0 \tag{15}$$

$$C_{ox}\left(\bar{x},t\right) = C_{ox}^s = 8.576\cdot 10^{-3} \text{ for } \bar{x} \in \Gamma \tag{16}$$

The values used in conditions (15) and (16) correspond to amount of dissolved oxygen in concrete mixed with typical fresh water (0.005 kg/m^3) and the quantity of dissolved oxygen at the concrete surface, when atmospheric air is saturated [9].

The diffusion coefficient D_{ox} is dependent on the degree of water content in the concrete. In wet concrete, oxygen diffuses in solution, while in partially-saturated concrete, oxygen diffuses partly through the gas phase and partly through the pore solution. To be consumed in the cathodic reaction, oxygen has to be in a dissolved state. The moisture distribution along the concrete cover will affect the amount of oxygen available at the reinforcement level, however, to simplify the analysis, a constant value of D_{ox} is used [9].

5. Propagation phase

Depending on oxidation degree the volumetric expansion of corrosion products may vary. Oxides created during the iron oxidation process, can take even 6 times greater volume than iron. When the volume of all corrosion products takes too much space, concrete cracks and a longitudinal crack appears. Taking into consideration that reduction of the rebar diameter can be neglected when compared to initial diameter, the mass of rust produced at anode is [9]

$$M_r = \frac{2.862 \cdot 10^{-7}}{r_m} \pi d i_{corr} \Delta t \tag{17}$$

where:

d – initial diameter [m],
r_m – steel-to-rust molecular weight ratio, 0.523 for $Fe(OH)_3$ or 0.622 for $Fe(OH)_2$,
Δt – time since the onset of steel depassivation in seconds,
i_{corr} – corrosion rate [A/m^2].

Considering the assumption of uniformly distributed corrosion, the relation between the change of volume and unit volume of reinforcement bar can be expressed as, [9]

$$\varepsilon_v = \frac{\Delta V}{V} = \frac{4M_r}{\pi d^2}\left(\frac{1}{\rho_r} - \frac{0.523}{\rho_s}\right) \tag{18}$$

where:

ρ_s – steel density,
ρ_r – rust density, $\rho_r = 1.96 \cdot 10^3$ kg/m^3.

The volumetric expansion of corrosion products results in the formation of internal pressure expressed by

$$p = \frac{\varepsilon_v E_r}{2(1+\nu_r)(1-2\nu_r)} \tag{19}$$

where:

E_r – elasticity modulus, $E_r = 12$ MPa,
$\nu_r = 0.499$ – Poisson ratio for rust.

6. Concrete cylinder model

The state of stress in the concrete surrounding reinforcement bar, a thick-walled cylinder model created by Bazant and Tepfers is used. The thickness of the ring is the shortest way to crack the concrete cover (c_y in fig. 3(a)). Concrete is assumed to be linearly elastic material. The stresses caused by rust expansion are treated as a homogeneous pressure and the problem of empty cylinder with axisymmetric load is considered in plane strain conditions. The stress in a thick-walled cylinder, with inner radius $d/2$ and outer radius $c + d/2$, under homogeneous pressure p, is expressed as [9]

$$\sigma_\theta = \frac{(d/2)^2 p}{(c+d/2)^2 - (d/2)^2}\left(1 + \frac{(c+d/2)^2}{r^2}\right) \tag{20}$$

where:

σ_θ – circumferential stress in concrete,
c – concrete cover thickness,
r – radius of the point where the stresses are determined.

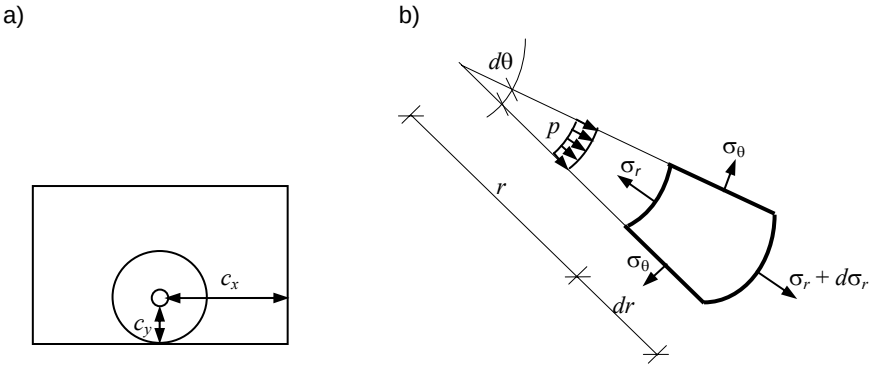

Fig. 3. Idealization of concrete cover as thick-walled cylinder: (a) cylider model, (b) stresses in axisymmetric concrete ring

Rys. 3. Idealizacja otuliny betonowej jako grubościennego cylindra: (a) model cylindra, (b) naprężenia w osiowo-symetrycznym betonowym pierścieniu

When the stress calculated from equation (20) is no longer balanced by the tensile strength of concrete f_{ctm}, an internal crack starts to form. In this situation two layers can be distinguished in the concrete ring: the inner part, in which the circumferential stresses have already exceeded f_{ctm}, and the outer part, in which concrete is still continuous elastic material and the stress values are below f_{ctm} (see fig. 4).

Until a crack develops, pressure p is carried by the outer layer and its value is reduced together with expansion of the cracked zone [9]. Using an analogy to uncracked ring, a new expressions for circumferential stress in the uncracked zone in the partly-cracked state can be written

$$\sigma_\theta = p\frac{d}{2e}\frac{e^2}{\left(c+d/2\right)^2-e^2}\left(1+\frac{\left(c+d/2\right)^2}{r^2}\right) \tag{21}$$

where:

e – length of crack (thickness of cracked zone).

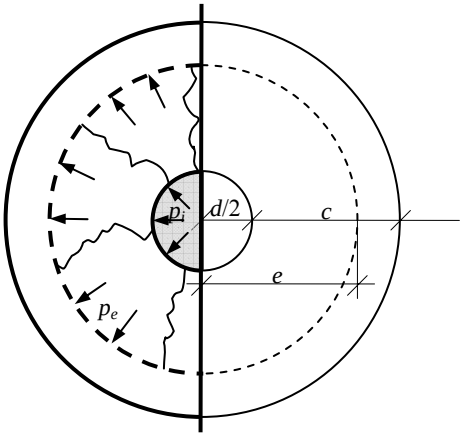

Fig. 4. Scheme of cracked and uncracked zones and definition of crack penetration depth e

Rys. 4. Schemat strefy zarysowanej i niezarysowanej oraz definicja głębokości penetracji rysy e

When the load carrying capacity of the concrete cylinder under tension is reached, cracks penetrate throughout the whole thickness revealing reinforcement.

According to [10] the relation between loss of diameter Δd and crack width Δw can be approximated by linear function, where proportionality depends on initial diameter d and concrete cover c, all expressed in mm

$$\Delta w = \left(\alpha - 1\right)\pi d\frac{d/2+c}{\left(d+c\right)c}\Delta d \tag{22}$$

where:

$\alpha = \rho_r/\rho_s$ – rust density to steel density ratio.

An empirical expression for loss of diameter can be used, however for proper use i_{corr} must be expressed in $\mu A/cm^2$ and Δt in years.

$$\Delta d = 0.023 i_{corr}\Delta t \tag{23}$$

7. Numerical procedure

The electrical potential distribution for chlorides is calculated according to equation (3) using finite difference equations. The diffusion potential value is updated in every time step according to actual ionic concentration.

For chloride and oxygen concentrations the cellular automata are used. The equation (4), as well as equation (14) can be effectively simulated by adopting a von Neumann neighbourhood with radius equal to 1 and the following rule of evolution [3, 4]

$$C_i^k = \varphi_0 C_i^{k-1} + \sum_{j=1}^{d} \left(\varphi_j^- C_{i-1,j}^{k-1} + \varphi_j^+ C_{i-1,j}^{k-1} \right) \tag{24}$$

where:

C_i^k – concentration of ions in cell i at time t_k,
d – number of dimensions ($d = 2$).

The values of the evolutionary coefficients must satisfy the following normality rule, required by the mass conservation law [3, 4]

$$\varphi_0 + \sum_{j=1}^{d} \left(\varphi_j^- + \varphi_j^+ \right) = 1 \tag{25}$$

To ensure the stability of the numerical procedure, the stability condition should be maximum 0.5 [3–5]

$$0.5 \geq \frac{\Delta t \cdot D_i}{\Delta x^2} \tag{26}$$

where:

Δt – time step,
D_i – diffusion coefficient for ionic species,
Δx – grid dimension.

The dimensions of the element's cross-section are 350 mm × 600 mm and it is reinforced with 25 mm diameter bars. The calculations are made with the grid dimension $\Delta x = 0.01$ m and time step $\Delta t = 1$ day. The initial chloride concentration is estimated as $C_0 = 1.7\%$ of cement mass at the surface of concrete. Free chloride concentration is calculated according to equation (2), where α and β parameters are equal to 0.81 and 1, respectively. The initial oxygen concentration is estimated as $C_{ox}^{\ s} = 8.576 \times 10^{-3}$ kg/m^3 and $C_{ox} = 0.005$ kg/m^3. The other parameters of concrete used in calculations are set in table 1. The procedure of propagation phase is made on the basis of model presented by [9]. However, additional calculations concerning crack width are made. The duration of propagation phase t_p is understood as the time to first cracking through the concrete cover. All calculations procedures are prepared by authors, using MATLAB software.

Table 1

Parameters of concrete used for calculations

Class of concrete	C25/30
Tensile strength [MPa]	2.68
Cement content [kg/m3]	449
Chloride diffusion coefficient [m2/s]	2.2×10^{-12}
Oxygen diffusion coefficient [m2/s]	1×10^{-12}

8. Results

The free chloride concentration distribution is shown in fig. 5. The concentration after reaching chloride threshold is pointed out with continuous line, while with a dotted line, a chloride threshold value is marked. The initiation time is assumed as the time when chloride concentration at the reinforcement level reaches the chloride threshold value. The threshold value is assumed to be 0.35% of cement mass. The initiation time is calculated to be 30 years. The initiation time may seem to be short when compared to experimental data, however it may result from high boundary condition value for chlorides and constant diffusion coefficient assumption, independent on time, moisture or environmental conditions.

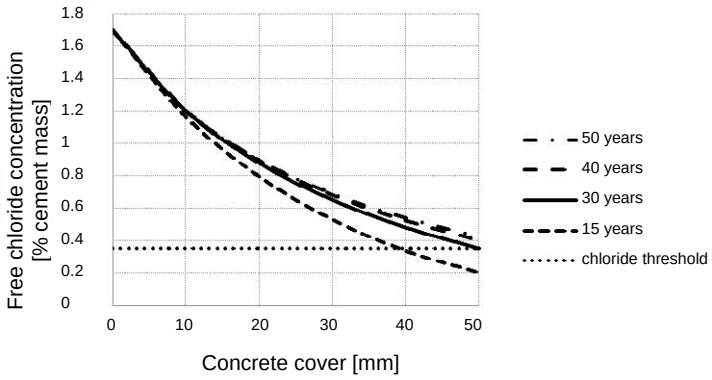

Fig. 5. Change of free chloride concentration in time with respect to chloride threshold value

Rys. 5. Zmiana stężenia wolnych chlorków w czasie z odniesieniem do wartości progowej

As the chloride concentration reaches chloride threshold value the corrosion initiation phase ends and the corrosion propagation phase begins. An oxygen concentration is calculated, as it limits the cathodic reaction. It is assumed that all oxygen available in cross-section is being consumed in reaction according to equation (15). To simplify the model, the dependency of oxygen diffusivity on moisture is neglected. The oxygen concentration distribution is shown in fig. 6.

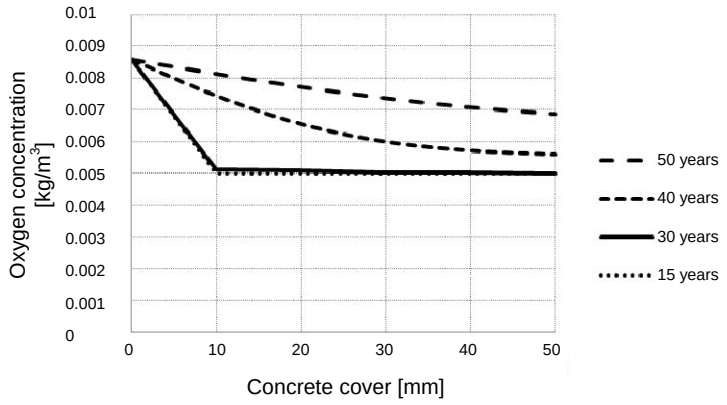

Fig. 6. Change of oxygen concentration in time

Rys. 6. Zmiana stężenia tlenu w czasie

The simulated change of corrosion current density during 7 years can be seen in fig. 7. According to equation (12) corrosion potential depends on cathode-to-anode area ratio A_c/A_a. In literature no precise value of this ratio can be found. Some authors neglect this relation [8], what is modelled using $A_c/A_a = 1$, while others specify it as a constant value $A_c/A_a = 10$ [9]. However due to character of corrosion phenomena, anode and cathode areas change in time, which suggest that also A_c/A_a varies in time, cf. [11]. Calculations proceed using three constant values of cathode-to-anode area ratio, $A_c/A_a = 1$; 5 or 10. For $A_c/A_a = 1$ corrosion increase much slower than for $A_c/A_a = 10$. After one year of propagation time, current calculated with $A_c/A_a = 1$ is still below 0.1 μA/cm^2, meaning no corrosion occurs, while current calculated with $A_c/A_a = 10$ is 0.3 μA/cm^2, which according to [9] responds to low corrosion rate.

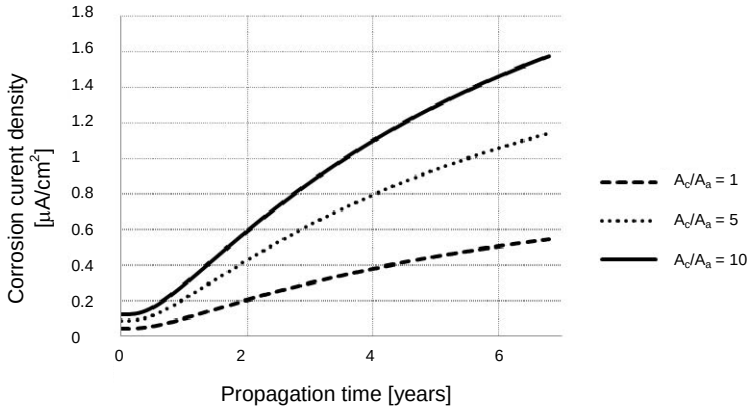

Fig. 7. Change of corrosion current density in time

Rys. 7. Zmiana gęstości prądu w czasie

Figure 8 shows the increase of crack length in time for three A_c/A_a ratios and for the 50 mm cover. As it could be expected from fig. 7 analysis, for current density with a A_c/A_a ratio equal to 1 cracking develops after one year, while for currents with higher A_c/A_a ratio cover is already cracked within that time. It can be noticed that there is some critical depth of crack, reaching which results in sudden crack length increase. In table 2 width of crack and reduction of reinforcement diameter due to corrosion can be found.

Considering the fact that the reduction of diameter is independent of the steel type, the crack width does not depend on it either. The crack width depends on the time to first cracking t_p, i_{corr} value and the initial reinforcement bar diameter. Despite the small initial crack width, it may increase with time and can become a significant parameter.

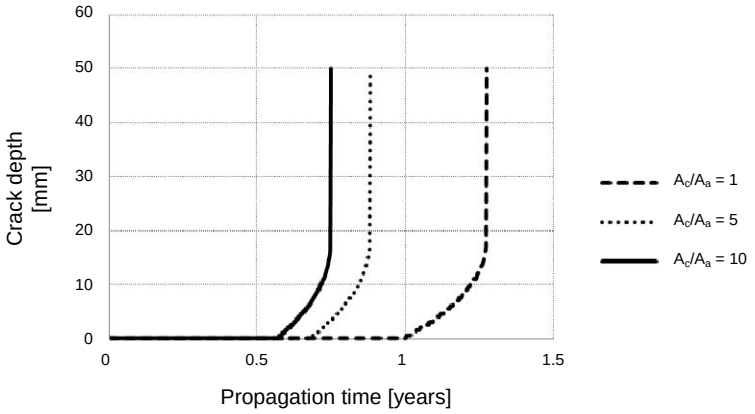

Fig. 8. Increase of crack length in time for 50 mm cover

Rys. 8. Przyrost długości rysy w czasie dla otuliny 50 mm

Table 2

Width of crack and loss of reinforcement diameter for 50mm cover

Concrete	Loss of diameter [mm]	Crack width [mm]
C25/30	3.74×10^{-3}	3.67×10^{-3}

9. Conclusions

The estimated duration of initiation phase is 30 years. It is the time in which the free chloride concentration reaches the chloride threshold value assumed to be 0.35% of cement mass (at the reinforcement level). The chloride binding is considered using Freundlich isotherm with α and β parameters equal to 0.81 and 1.

The time of propagation phase (i.e. time to first cracking) depends on actual corrosion current density and cover depth. It decreases with the increase of current density. Oxygen concentration calculations assume constant diffusion coefficient. The anodic and cathodic reactions considers activation and concentration polarization. For corrosion current density calculations, three anode-to-cathode areas ratios are assumed to be constant values. The

higher anode-to-cathode ratio is, the higher corrosion current density values are, which results in lower time to first cracking. The crack width is insignificant considering the mechanical properties of RC element, however its increase changes the chloride ion transportation model and concrete can no longer be treated as a protecting cover.

The simplifications used in model proposed are going to be considered in future research. Not only should the linear relation between C_b and C_f be considered, but also the nonlinear one ($\beta < 1$). Oxygen diffusion may be considered moisture dependent and the concrete resistivity could be included instead of assuming constant anode-to-cathode areas ratio [11]. However this was a consequence of ignoring the longitudinal direction of element.

The chloride corrosion of reinforcement is a perfect example of a destructive action of environment on a RC structure. Treating corrosion as a factor that initiates cracking, its analysis can also be the starting point for further considerations within fracture mechanics.

References

[1] Stanish K., Hooton R.D., Thomas M.D.A., *A novel method for describing chloride ion transport due to an electrical gradient in concrete: Part 1. Theoretical description*, Cement and Concrete Research 34, 2004, 43-49.

[2] Samson E., Marchand J., Beaudoin J.J., *Describing ion diffusion mechanisms in cement-based materials using the homogenization technique*, Cement and Concrete Research 29, 1999, 1341-1345.

[3] Biondini F., Bontempi F., Frangopol D.M., Malerba P.G., *Cellular automata approach to durability analysis of concrete structures in aggressive environments*, Journal of Structural Engineering, Vol. 130, No. 11, 2004, 1724-1737.

[4] Zaborski A., *Concrete elements durability in aggressive environments: cellular automata simulation*, Environmental Effects on Buildings, Structures, Materials and People, Lublin University of Technology, 2007, 303-312.

[5] Nielsen E., Geiker M.R., *Chloride diffusion in partially saturated cementitious material*, Cement and Concrete Research 33, 2002, 133-138.

[6] Zybura A., *Zabezpieczenie konstrukcji żelbetowych metodami elektrochemicznymi*, monograph, Silesian University of Technology, 2003.

[7] Krykowski T., Zybura A., *FEM modelling of concrete degradation caused by rebar corrosion in reinforced concrete*, Architecture Civil Engineering Environment 4, 2009, 71-80.

[8] Jaśniok T., *Identyfikacja szybkości korozji zbrojenia elementów żelbetowych na podstawie pomiarów polaryzacyjnych*, PhD thesis, Faculty of Civil Engineering, Silesian University of Technology, 2004.

[9] Martin-Perez B., *Service life modelling of RC highway structures exposed to chlorides*, PhD thesis, Department of Civil Engineering, University of Toronto.

[10] Thoft-Christensen P., *Corrosion and cracking of reinforced*, Life cycle performance of deterioration structures, ASCE 2003, 26-36.

[11] Klakocar-Ciepacz M., *Doświadczalne modelowanie ogniwa korozyjnego w żelbecie*, PhD thesis, Faculty of Chemistry, Wrocław University of Technology, 1999.